

Diagonal boundary conditions in critical loop models

Max Downing, Jesper Lykke Jacobsen, Rongvoram Nivesvivat, Sylvain Ribault, Hubert Saleur

(JJ, SR, HS) Institut de physique théorique, CEA, CNRS, Université Paris-Saclay

(MD, JJ) Laboratoire de Physique de l'École Normale Supérieure, ENS, Université PSL, CNRS, Sorbonne Université, Université Paris Cité, Paris, France

(RN) New York University Abu Dhabi, United Arab Emirates

(HS) Department of Physics and Astronomy, University of Southern California, Los Angeles

E-mail: max.downing@phys.ens.fr, jesper.jacobsen@ens.fr, rongvoramnivesvivat@gmail.com, sylvain.ribault@ipht.fr, hubert.saleur@ipht.fr

ABSTRACT: In critical loop models, we define diagonal boundaries as boundaries that couple to diagonal fields only. Using analytic bootstrap methods, we show that diagonal boundaries are characterised by one complex parameter, analogous to the boundary cosmological constant in Liouville theory. We determine disc 1-point functions, and write an explicit formula for disc 2-point functions as infinite combinations of conformal blocks.

For a discrete subset of values of the boundary parameter, the boundary spectrum becomes discrete, and made of degenerate representations. In such cases, we check our results by numerically bootstrapping disc 2-point functions.

We sketch the interpretation of diagonal boundaries in lattice loop models. In particular, a loop can neither end on a diagonal boundary, nor change weight when it touches it. In bulk-to-boundary OPEs, numbers of legs can be conserved, or increase by even numbers.

Contents

1	Introduction and summary	2
2	Boundary conditions and degenerate fields	6
2.1	Structure constants of the bulk CFT	7
2.2	Diagonal and non-diagonal boundary conditions	8
2.3	Disc 1-point functions	10
2.4	Modular bootstrap on the annulus	12
3	Bulk 2-point functions on the disc	13
3.1	Bulk channel decomposition	13
3.2	Boundary channel decomposition	15
3.3	Numerical bootstrap results	15
4	Outlook	18
	Acknowledgements	21
	References	22

1 Introduction and summary

In two-dimensional statistical physics, ensembles of non-intersecting loops can describe interesting phenomena including percolation or the physics of polymers, while being accessible to powerful methods such as integrable lattice techniques, see [1] for a review. In the critical limit, loop models give rise to conformal field theories (CFTs), and exact results can be derived using either algebraic CFT methods [1, 2], or probabilistic descriptions in terms of Schramm–Loewner evolutions [2, 3] or Conformal Loop Ensembles [4]. More recently, analytic bootstrap methods have led to much progress on correlation functions in critical loop models [5], including analytic formulas for a large number of structure constants [6, 7]. Nevertheless, critical loop models remain far from being solved, and even basic structural properties, such as the existence of operator product expansions, remain mysterious.

Boundary critical loop models

In this work we start applying the same bootstrap methods to critical loop models on surfaces with boundaries. Well-know results about boundary critical loop models include:

- Cardy’s computation of the probability that a cluster in critical percolation connects two disjoint arcs on the boundary, based on the determination of a boundary 4-point function [8].
- Schramm’s computation of the probability that a percolation hull running between two distinct boundary points passes to the left of a given bulk point, based on the determination of a correlation function between 2 boundary points and 1 bulk point [9].

We expect that there exist a variety of fields and boundary conditions, leading to many more correlation functions, and therefore many more interesting observables. In particular, we will determine a family of disc 2-point functions (1.12), which depend not only on the central charge, like Cardy's and Schramm's results, but also on parameters that characterise boundary conditions and bulk fields. Our disc 2-point functions (1.12) are infinite combinations of conformal blocks, whereas Cardy's and Schramm's probabilities are simple hypergeometric conformal blocks.

The technical contents of this work rely exclusively on the bootstrap method, and only rarely do we need hints from statistical loop models, be it on the lattice or in the continuum limit. We therefore consider critical loop models as CFTs characterised, in particular, by their bulk primary fields. In the Outlook, Section 4, we will sketch the meaning of some of our results in lattice loop models, which we plan to discuss in more detail in future works.

In this text we assume familiarity with 2d boundary CFT and with critical loop models on the sphere. On 2d boundary CFT, we recommend the classic work of Lewellen [10]. On critical loop models on the sphere, we recommend the recent review [5].

Boundary conditions: diagonal or non-diagonal

Introducing boundaries immediately raises the issue of choosing boundary conditions. In the bootstrap approach, once the bulk theory is given, the boundary parameters are the structure constants left undetermined by the bootstrap equations. (We call structure constant the coefficient of a conformal block in the decomposition of a correlation function.) In critical loop models, the bulk theory has 3 types of primary fields, characterised by their left and right conformal dimensions, whose difference is the conformal spin:

Name	Notation	Conditions	(P, \bar{P})	Spin
Degenerate	$V_{(1,s)}^d$	$s \in \mathbb{N}^*$	$(P_{(1,s)}, P_{(1,s)})$	0
Diagonal	V_P	$P \in \mathbb{C}$	(P, P)	0
Non-diagonal	$V_{(r,s)}$	$r \in \frac{1}{2}\mathbb{N}^*, s \in \frac{1}{r}\mathbb{Z}$	$(P_{(r,s)}, P_{(r,-s)})$	rs

(1.1)

We use the following notations for the central charge c and conformal dimension Δ :

$$c = 13 - 6\beta^2 - 6\beta^{-2} \quad , \quad \Delta = \frac{c-1}{24} + P^2 \quad , \quad P_{(r,s)} = \frac{1}{2}(\beta r - \beta^{-1}s) \quad , \quad (1.2)$$

where P is the momentum and r, s are Kac indices. The central charge is a complex number obeying $\Re c < 13 \iff \Re \beta^2 > 0$. Similarly, we will write $\psi_{(r,s)}^d$ for a degenerate boundary field with Kac indices $r, s \in \mathbb{N}^*$.

The existence of degenerate fields allows us to use the analytic bootstrap method. This method is based on solving crossing symmetry equations for correlation functions that involve the simplest nontrivial degenerate field $V_{(1,2)}^d$, whose OPEs with non-degenerate fields read

$$V_{(1,2)}^d V_P \sim \sum_{\pm} C_P^{\pm} V_{P \pm \frac{1}{2\beta}} \quad , \quad V_{(1,2)}^d V_{(r,s)} \sim \sum_{\pm} C_{(r,s)}^{\pm} V_{(r,s \pm 1)} \quad . \quad (1.3)$$

In these OPEs we write only primary fields and omit descendants, while C_P^{\pm} and $C_{(r,s)}^{\pm}$ are OPE coefficients. The resulting analytic bootstrap constraints determine how correlation functions behave under $P \rightarrow P + \beta^{-1}$ or $s \rightarrow s + 2$.

Due to crossing symmetry of the disc 2-point function $\langle V_{(1,2)}^d V_{(r,s)} \rangle$, the disc 1-point structure constant $\langle V_{(r,s)} \rangle$ obeys an equation of the type

$$\mu \langle V_{(r,s)} \rangle = \sum_{\pm} C_{(r,s)}^{\pm} f_{(r,s)}^{\pm} \langle V_{(r,s\pm 1)} \rangle . \quad (1.4)$$

(See Section 2.2 for more details.) Here $f_{(r,s)}^{\pm}$ (2.14) are fusion matrix elements, and μ is the bulk-to-boundary OPE coefficient defined by

$$V_{(1,2)}^d \rightarrow \mu \psi_{(1,1)}^d + \tilde{\mu} \psi_{(1,3)}^d , \quad (1.5)$$

where $\psi_{(1,1)}^d$ is the boundary identity field, and $\psi_{(1,3)}^d$ is a degenerate boundary field. By conformal invariance, $\langle V_{(r,s)} \rangle$ must vanish unless the conformal spin rs vanishes, so that

$$\langle V_{(r,s \neq 0)} \rangle = 0 . \quad (1.6)$$

Combining this constraint with the case $s = 0$ of Eq. (1.4), we obtain

$$\mu \langle V_{(r,0)} \rangle = 0 . \quad (1.7)$$

This leads us to distinguish 2 types of boundary conditions:

- **Diagonal boundary conditions**, such that $\mu \neq 0$, therefore $\langle V_{(r,s)} \rangle = 0$: only diagonal or degenerate fields (V_P or $V_{(1,s)}^d$) have non-zero disc 1-point functions.
- **Non-diagonal boundary conditions**, such that $\mu = 0$, so that spinless non-diagonal fields $V_{(r,0)}$ can also have non-zero disc 1-point functions.

In this work we focus on diagonal boundaries. A diagonal boundary is characterised by the disc 1-point functions of diagonal fields $\langle V_P \rangle$, which also determines $\langle V_{(1,s)}^d \rangle$. Crossing symmetry of the disc 2-point function $\langle V_{(1,2)}^d V_P \rangle$ implies the equation

$$\mu \langle V_P \rangle = \sum_{\pm} \langle V_{P \pm \frac{1}{2\beta}} \rangle . \quad (1.8)$$

In contrast to Eq. (1.4), the right-hand side of this equation has trivial coefficients: this is achieved by an appropriate field renormalisation. (See Section 2.1 for more details.) As we will show in Section 2.3, the solutions that are relevant to critical loop models are

$$\langle V_P \rangle_{\sigma} = \sin(4\pi\sigma P) \quad , \quad \mu_{\sigma} = 2 \cos(2\pi\beta^{-1}\sigma) , \quad (1.9)$$

for any choice of the boundary parameter $\sigma \in \mathbb{C}$. These solutions formally coincide with disc 1-point functions in Liouville theory with $c \leq 1$ [11], although loop models exist in the larger domain $\Re c < 13$. In Liouville theory with a generic $c \in \mathbb{C} \setminus (-\infty, 1)$, the relevant solution is a cos instead of a sin (2.23), and μ_{σ} is the boundary cosmological constant [12].

Boundary conditions: discrete or continuous

For our numerical bootstrap methods to work, the bulk-to-boundary OPEs of any bulk field should give rise to a discrete combination of boundary fields. If this holds, we will say that we have a **discrete boundary**; if not, a **continuous boundary**. In bulk loop models, OPEs are discrete. This does not imply that all boundaries are discrete: for

example, the compactified free boson has finite bulk OPEs, but some of its boundaries are continuous [13]. We propose the following (conjectural) criterion, which allows us to easily deduce the discrete values of σ from the solution (1.9):

$$\text{Discrete boundary} \begin{array}{c} \xleftrightarrow{\text{criterion}} \\ \end{array} \mu_\sigma = \frac{\langle V_{P_{(1,2)}} \rangle_\sigma}{\langle V_{P_{(1,1)}} \rangle_\sigma} \begin{array}{c} \xleftrightarrow{\text{explicitly}} \\ \end{array} \sigma \in \{P_{(0,S)}\}_{S \in \mathbb{N}^*}. \quad (1.10)$$

where $P_{(r,s)}$ was defined in Eq. (1.2). (See Section 2.3 for a justification.) We can also deduce the boundary spectrum from the disc 1-point function, using modular covariance of the annulus (= cylinder) partition function. We find in Section 2.4 that the boundary spectrum is discrete if and only if the boundary is discrete. For a discrete boundary with parameter $S \in \mathbb{N}^*$, the boundary spectrum is made of degenerate boundary fields,

$$\mathcal{S}_S = \left\{ \psi_{\langle r,s \rangle}^d \right\}_{\substack{r \in \mathbb{N}^* \\ s=1,3,\dots,2S-1}}. \quad (1.11)$$

Bulk 2-point function: bulk channel decomposition

From the disc 1-point function, we could deduce any bulk N -point function on the disc using bulk OPEs [10]. However, in critical loop models, we know bulk 3-point functions [7], but we do not know bulk OPEs. This will not prevent us from computing bulk 2-point functions on the disc. In this case, we only need to perform the bulk OPE once, and to focus on contributions from diagonal fields, since our boundary is diagonal. Known results from the bulk CFT suggest that diagonal fields contribute to the bulk OPE with OPE coefficients that coincide with 3-point functions [6]. The bulk OPE therefore leads to an explicit conjecture for the bulk channel decomposition of the bulk 2-point function,

$$\langle V_{(r_1,s_1)} V_{(r_2,s_2)} \rangle_\sigma = \sum_{P \in P_0 + \beta^{-1}\mathbb{Z}} C_{(r_1,s_1)(r_2,s_2)}^P \langle V_P \rangle_\sigma \quad (1.12)$$

(See Section 3.1 for more details.) We implicitly assume $r_1 + r_2 \in \mathbb{N}$, otherwise the 2-point function vanishes due to the conservation of r modulo integers in the bulk CFT. The diagram represents a t -channel Virasoro conformal block, as determined by the standard mirror relation

$$\left\langle V_1(z_1) V_2(z_2) \right\rangle_{\text{conformal blocks}} = \left\langle V_{P_1}(z_1) V_{\bar{P}_1}(\bar{z}_1) V_{P_2}(z_2) V_{\bar{P}_2}(\bar{z}_2) \right\rangle_{\text{sphere}}. \quad (1.13)$$

In the decomposition (1.12), the bulk channel spectrum depends on a momentum $P_0 \in \mathbb{C}$: this parameter characterises a bulk combinatorial defect [14]. The disc 1-point function $\langle V_P \rangle_\sigma$ comes from Eq. (1.9), and the bulk OPE coefficient is

$$C_{(r_1,s_1)(r_2,s_2)}^P = \frac{-16P \prod_{\pm} \sin(\pi\beta^{\pm 2}) \Gamma_{\beta}(\pm 2P)}{\prod_{\epsilon_1, \epsilon_2, \epsilon_3 = \pm} \Gamma_{\beta} \left(\frac{\beta + \beta^{-1}}{2} + \frac{\beta}{2} |\epsilon_1 r_1 + \epsilon_2 r_2| + \frac{\beta^{-1}}{2} (\epsilon_1 s_1 + \epsilon_2 s_2) + \epsilon_3 P \right)}, \quad (1.14)$$

where Γ_{β} is the Barnes double Gamma function.

Bulk 2-point function: boundary channel decomposition

In order to test our bulk channel decomposition of the bulk 2-point function, let us compare it with the boundary channel decomposition of the same quantity,

$$\langle V_{(r_1, s_1)} V_{(r_2, s_2)} \rangle_\sigma = \sum_{k \in \mathcal{S}_\sigma} D_k \begin{array}{ccc} (r_1, s_1) & & (r_2, s_2) \\ & \diagdown \quad \diagup & \\ & k & \\ & \diagup \quad \diagdown & \\ (r_1, -s_1) & & (r_2, -s_2) \end{array} \quad (1.15)$$

where \mathcal{S}_σ and D_k are the boundary channel spectrum and structure constants. We have no control over the structure constants, but in the discrete case we know the spectrum $\mathcal{S}_{\sigma=P_{(0,S)}} = \mathcal{S}_S$ (1.11), and this is enough for testing the bulk channel decomposition. The decomposition passes the test, and we also find that many structure constants D_k vanish. In other words, the boundary channel spectrum of $\langle V_{(r_1, s_1)} V_{(r_2, s_2)} \rangle_S$ is not the full spectrum \mathcal{S}_S , but only the subset

$$\mathcal{S}_S^{r_1, r_2} = \{ \psi_{\langle r, s \rangle}^d \}_{r \in 2\max(r_1, r_2) + 1 + 2\mathbb{N}, s=1, 3, \dots, 2S-1} \quad (1.16)$$

(See Section 3.2 for more details.) This suggests bulk-to-boundary OPEs of the type

$$V_{(r_1, s_1)} \rightarrow \sum_{r \stackrel{\Delta}{=} 2r_1 + 1}^{\infty} \sum_{s \stackrel{\Delta}{=} 1}^{2S-1} \psi_{\langle r, s \rangle}^d, \quad (1.17)$$

where the sums run by increments of 2. Such OPEs are consistent with the fusion rules of the degenerate fields $\psi_{\langle r, s \rangle}^d$, more specifically with the fusion product $\psi_{\langle r, s \rangle}^d \times V_{(r_1, s_1)} \supset V_{(r_1, -s_1)}$ that is relevant to our s -channel conformal block in Eq. (1.15). These OPEs are also consistent with the statistical model interpretation of the bulk and boundary fields as punctures, with a number of legs that depends on the first Kac index:

$$(1.18)$$

This interpretation is already well-known in the cases of $V_{(r,s)}$ [15] and $\psi_{\langle r, 1 \rangle}^d$ [2]. It implies that in the bulk-to-boundary OPEs (1.17), the number of legs can be conserved, or increased by even numbers, but not decreased: this shows that diagonal boundaries cannot absorb legs. (In bulk OPEs, numbers of legs are conserved modulo even integers, but they can decrease [6].) We conclude that loops cannot end on a diagonal boundary, except at a boundary field.

2 Boundary conditions and degenerate fields

The structure and solvability of a 2d CFT depends crucially on the existence of degenerate fields. In Liouville theory and A- and D-series minimal models, the existence of two independent degenerate fields $V_{\langle 2, 1 \rangle}^d$ and $V_{\langle 1, 2 \rangle}^d$, leads to a complete solution via the analytic bootstrap method. In critical loop models, we have only $V_{\langle 1, 2 \rangle}^d$, which is a priori not enough for uniquely determining correlation functions [5]. Nevertheless, we find that diagonal boundary conditions are solvable, and lead to disc 1-point functions that are very similar to those of Liouville theory.

2.1 Structure constants of the bulk CFT

We first make a brief detour via the bulk CFT, in order to derive field normalisations such that the shift equation (1.8) for the disc 1-point function has trivial coefficients.

In fact, the required normalisations also simplify the shift equation for the sphere 2-point structure constant $B_k \propto \langle V_k V_k \rangle^{\text{sphere}}$. Consider the s - and t -channel decompositions of the following sphere 4-point function:

$$\begin{aligned}
 \langle V_{\langle 1,2 \rangle} V_{\langle 1,2 \rangle} V_P V_P \rangle^{\text{sphere}} &= \frac{B_{\langle 1,2 \rangle} B_P}{B_{\langle 1,1 \rangle}} \left| \begin{array}{c} \langle 1,2 \rangle \quad P \\ \diagdown \quad \diagup \\ \langle 1,1 \rangle \\ \diagup \quad \diagdown \\ \langle 1,2 \rangle \quad P \end{array} \right|^2 + \tilde{D}_{\langle 1,3 \rangle} \left| \begin{array}{c} \langle 1,2 \rangle \quad P \\ \diagdown \quad \diagup \\ \langle 1,3 \rangle \\ \diagup \quad \diagdown \\ \langle 1,2 \rangle \quad P \end{array} \right|^2, \\
 &= \sum_{\pm} (C_P^{\pm})^2 B_{P \pm \frac{1}{2\beta}} \left| \begin{array}{c} \langle 1,2 \rangle \quad P \\ \diagdown \quad \diagup \\ P \pm \frac{1}{2\beta} \\ \diagup \quad \diagdown \\ \langle 1,2 \rangle \quad P \end{array} \right|^2. \tag{2.1}
 \end{aligned}$$

In addition to B_k , these decompositions involve the degenerate OPE coefficients C_P^{\pm} (1.3) and a structure constant $\tilde{D}_{\langle 1,3 \rangle}$. The diagrams denote s - and t -channel Virasoro conformal blocks, and the modulus squared means that we take products of left-moving blocks (functions of the cross-ratio z of the 4 fields' positions) with right-moving blocks (functions of \bar{z}). The s - and t -channel blocks are linearly related,

$$\left| \begin{array}{c} \langle 1,2 \rangle \quad P \\ \diagdown \quad \diagup \\ P \pm \frac{1}{2\beta} \\ \diagup \quad \diagdown \\ \langle 1,2 \rangle \quad P \end{array} \right|^2 = f_P^{\pm} \left| \begin{array}{c} \langle 1,2 \rangle \quad P \\ \diagdown \quad \diagup \\ \langle 1,1 \rangle \\ \diagup \quad \diagdown \\ \langle 1,2 \rangle \quad P \end{array} \right|^2 + \tilde{f}_P^{\pm} \left| \begin{array}{c} \langle 1,2 \rangle \quad P \\ \diagdown \quad \diagup \\ \langle 1,3 \rangle \\ \diagup \quad \diagdown \\ \langle 1,2 \rangle \quad P \end{array} \right|^2, \tag{2.2}$$

where $f_P^{\pm}, \tilde{f}_P^{\pm}$ are fusion matrix elements which can be found in [5]. We will only need the explicit form of

$$f_P^{\pm} = \frac{\Gamma(2\beta^{-2} - 1)\Gamma(1 \pm 2P\beta^{-1})}{\Gamma(2\beta^{-2})\Gamma(\beta^{-2} \pm 2P\beta^{-1})}. \tag{2.3}$$

Inserting this relation in Eq. (2.1), and considering the coefficient of $\left| \begin{array}{c} \langle 1,2 \rangle \quad P \\ \diagdown \quad \diagup \\ \langle 1,1 \rangle \\ \diagup \quad \diagdown \\ \langle 1,2 \rangle \quad P \end{array} \right|^2$, we

obtain a shift equation for B_P ,

$$\frac{B_{\langle 1,2 \rangle} B_P}{B_{\langle 1,1 \rangle}} = \sum_{\pm} (C_P^{\pm} f_P^{\pm})^2 B_{P \pm \frac{1}{2\beta}}. \tag{2.4}$$

We slightly simplify this equation by normalising the fields such that $B_{\langle 1,1 \rangle} = 1$. This is a natural choice of normalisation since $V_{\langle 1,1 \rangle}^d$ is the bulk identity field. A further simplification occurs if we choose field normalisations such that

$$C_P^{\pm} = (f_P^{\pm})^{-1}. \tag{2.5}$$

And indeed, this identity is obeyed if we start from the normalisations of [5], and perform the field renormalisation $V_k \rightarrow \lambda_k V_k$ so that $C_P^\pm \rightarrow \frac{\lambda_{(1,2)} \lambda_P}{\lambda_{P \pm \frac{1}{2\beta}}} C_P^\pm$, with

$$\lambda_{(1,2)} = \beta^{-\beta^{-2}}, \quad \lambda_P = 16P \prod_{\pm} \sin(2\pi\beta^{\pm 1}P) \Gamma_{\beta}(\pm 2P). \quad (2.6)$$

In the normalisation of [5], diagonal fields are even $V_P = V_{-P}$. Since $\lambda_P = -\lambda_{-P}$, our renormalisation makes them odd,

$$V_P = -V_{-P}. \quad (2.7)$$

Furthermore, since λ_P is invariant under $\beta \rightarrow \beta^{-1}$, the shift equation from the 4-point function $\langle V_{(2,1)}^d V_{(2,1)}^d V_P V_P \rangle^{\text{sphere}}$ also simplifies (assuming $V_{(2,1)}^d$ exists), and the two shift equations read

$$B_{(2,1)} B_P = \sum_{\pm} B_{P \pm \frac{\beta}{2}}, \quad B_{(1,2)} B_P = \sum_{\pm} B_{P \pm \frac{1}{2\beta}}. \quad (2.8)$$

The solution of these shift equations is

$$B_P = - \prod_{\pm} \frac{\sin(2\pi\beta^{\pm 1}P)}{\sin(\pi\beta^{\pm 2})} \quad \text{with} \quad \begin{cases} B_{(2,1)} = -2 \cos(\pi\beta^2), \\ B_{(1,2)} = -2 \cos(\pi\beta^{-2}). \end{cases} \quad (2.9)$$

This solution is only unique up to a P -independent prefactor, which we have chosen such that $B_{P_{(1,1)}} = 1$, consistently with the identification $B_{(1,1)} = B_{P_{(1,1)}}$. Then we also have $B_{(2,1)} = B_{P_{(2,1)}}$ and $B_{(1,2)} = B_{P_{(1,2)}}$.

Our expression for the bulk 2-point structure constant of diagonal fields B_P is valid in critical loop models, and also in Liouville theory with $c \leq 1$. And indeed it can alternatively be derived from the known structure constants of these theories, by applying a field renormalisation such that our normalization condition (2.5) is obeyed.

2.2 Diagonal and non-diagonal boundary conditions

Here we derive the shift equation (1.4) for the disc 1-point function $\langle V_{(r,s)} \rangle$. We begin by justifying the bulk-to-boundary OPE of the degenerate field $V_{(1,2)}^d$ (1.5). The vanishing of that field's singular vector implies that its bulk-to-boundary OPE produces boundary fields with momenta $P_{(1,1)}$ and $P_{(1,3)}$: this can be seen using Ward identities or equivalently BPZ equations. But does this OPE produce the degenerate fields $\psi_{(1,1)}^d$ and $\psi_{(1,3)}^d$, or the non-degenerate fields $\psi_{P_{(1,1)}}$, $\psi_{P_{(1,3)}}$? In the bulk CFT, the analogous question about the OPE $V_{(1,2)}^d V_{(1,2)}^d$ is easily answered using OPE associativity, and the fact that a field is degenerate if and only if its OPE with any other primary field produces finitely many primary fields [5]. The same argument would show that the set of boundary degenerate fields is closed under OPEs, but it does not work for bulk-to-boundary OPEs. In that case, we can resort to the pedestrian argument of solving the BPZ equation for the disc correlation function $\langle V_{(1,2)}^d \psi_{p_1} \psi_{p_2} \rangle$, where ψ_p is a primary boundary field of momentum $p \in \mathbb{C}$. This correlator on the disc satisfies the same Ward identities as a sphere 4-point function of four holomorphic fields. Two of the fields in the sphere 4-point function are degenerate, hence we have two second-order BPZ equations. We find that the compatibility of these two BPZ equations implies

$$\prod_{\pm} (p_1 \pm p_2) \prod_{\pm, \pm} (p_1 \pm p_2 \pm \beta^{-1}) = 0. \quad (2.10)$$

This is equivalent to $\langle \psi_{\langle 1,1 \rangle}^d \psi_{p_1} \psi_{p_2} \rangle \neq 0$ or $\langle \psi_{\langle 1,3 \rangle}^d \psi_{p_1} \psi_{p_2} \rangle \neq 0$, which shows that the bulk-to-boundary OPE of $V_{\langle 1,2 \rangle}^d$ produces degenerate fields.

We now consider the disc 2-point function $\langle V_{\langle 1,2 \rangle}^d V_{(r,s)} \rangle$, and decompose it in both the bulk and boundary channels, according to the bulk and bulk-to-boundary OPEs (1.3) and (1.5). Schematically,

$$\begin{array}{ccc}
 \text{bulk channel} & & \text{boundary channel} \\
 \text{(1.1)} & & \text{(1.2)}
 \end{array}
 \tag{2.11}$$

This leads to two decompositions of $\langle V_{\langle 1,2 \rangle}^d V_{(r,s)} \rangle$ into conformal blocks,

$$\begin{aligned}
 \langle V_{\langle 1,2 \rangle}^d V_{(r,s)} \rangle &= \mu \langle V_{(r,s)} \rangle + \tilde{d}_{\langle 1,3 \rangle} \langle V_{(r,s)} \rangle, \\
 &= \sum_{\pm} C_{(r,s)}^{\pm} \langle V_{(r,s\pm 1)} \rangle,
 \end{aligned}
 \tag{2.12}$$

where μ is defined in Eq. (1.5), and $\tilde{d}_{\langle 1,3 \rangle}$ is a boundary channel 2-point structure constant. The conformal blocks in the two channels are related by a linear transformation of the type

$$\langle V_{(r,s\pm 1)} \rangle = f_{(r,s)}^{\pm} \langle V_{(r,s)} \rangle + \tilde{f}_{(r,s)}^{\pm} \langle V_{(r,s)} \rangle,
 \tag{2.13}$$

where the fusion matrix elements $f_{(r,s)}^{\pm}$ are (see [5])

$$f_{(r,s)}^{\pm} = \frac{\Gamma(2\beta^{-2} - 1)\Gamma(1 \mp 2P_{(r,s)}\beta^{-1})}{\Gamma(\beta^{-2} \mp r)\Gamma((1 \pm s)\beta^{-2})}.
 \tag{2.14}$$

Projecting the crossing symmetry equation (2.12) on the boundary identity channel, we obtain the shift equation (1.4) for the disc 1-point function.

We have seen in Section 1 how the special case $r = 0$ of the shift equation leads to the distinction between diagonal and non-diagonal boundary conditions. Non-diagonal boundary conditions obey $\langle V_{(r,0)} \rangle \neq 0$ and $\langle V_{(r,s \neq 0)} \rangle = 0$; let us check that this is compatible with the general case of the shift equation. For $s \notin \{-1, 0, 1\}$ all three 1-point

functions in (1.4) vanish, so (1.4) contains no information in these cases. The case $s = 0$ is (1.7). Finally for $s = \mp 1$ we obtain the non-trivial relation

$$0 = C_{(r,\mp 1)}^\pm f_{(r,\mp 1)}^\pm \langle V_{(r,0)} \rangle. \quad (2.15)$$

From Eq. (2.14) we see that $f_{(r,\mp 1)}^\pm = 0$, so this equation is automatically obeyed, and does not constrain $\langle V_{(r,0)} \rangle$.

2.3 Disc 1-point functions

Let us derive shift equations for the disc 1-point functions of diagonal fields $\langle V_P \rangle$. We decompose the disc 2-point function $\langle V_{(1,2)}^d V_P \rangle$ in both the bulk and boundary channels, just like we did for $\langle V_{(1,2)}^d V_{(r,s)} \rangle$ in Eq. (2.12). The conformal blocks that appear are the same as for the 4-point function $\langle V_{(1,2)}^d V_{(1,2)}^d V_P V_P \rangle^{\text{sphere}}$ (2.1). The resulting shift equation (1.8) has trivial coefficients on the right-hand side, due to our choice of a field normalisation such that the bulk OPE coefficients and fusion matrix elements are related by Eq. (2.5).

Let us now solve the shift equation (1.8), together with the parity constraint $\langle V_P \rangle = -\langle V_{-P} \rangle$ which follows from Eq. (2.7). Given a value of μ and a number σ_0 such that $\mu_{\sigma_0} = \mu$, the general solution is

$$\langle V_P \rangle = \sum_{\sigma \in \sigma_0 + \beta \mathbb{Z}} c_\sigma \sin(4\pi\sigma P) \quad \text{with} \quad c_\sigma \in \mathbb{C}, \quad (2.16)$$

where the sum is over the set of solutions of $\mu_\sigma = \mu$. The existence of such a large space of solutions is due to the absence of a second degenerate field $V_{(2,1)}^d$, which would give rise to a second shift equation:

$$\tilde{\mu} \langle V_P \rangle = \sum_{\pm} \langle V_{P \pm \frac{\beta}{2}} \rangle. \quad (2.17)$$

In bulk critical loop models, the absence of $V_{(2,1)}^d$ also leads to large spaces of solutions. But in the case of the 3-point function of diagonal fields $\langle V_{P_1} V_{P_2} V_{P_3} \rangle^{\text{sphere}}$, we know that the correct solution obeys two shift equations, and therefore coincides with the 3-point function of $c \leq 1$ Liouville theory. This motivates

Main assumption: In the presence of a diagonal boundary, disc 1-point functions obey two shift equations.

Solutions of both shift equations are of the type (1.9), i.e. the infinite linear combination (2.16) reduces to one non-vanishing term. This obeys the second shift equation with $\tilde{\mu} = 2 \cos(2\pi\beta\sigma)$. The only remaining ambiguities come from rescalings $\langle V_P \rangle_\sigma \rightarrow N_\sigma \langle V_P \rangle_\sigma$, where N_σ is a P -independent factor.

We can also compute disc 1-point functions of degenerate fields. Since $V_{(1,1)}^d$ and $\psi_{(1,1)}^d$ are respectively the bulk and boundary identity fields, the bulk-to-boundary coefficient μ (1.5) may be rewritten as

$$\mu = \frac{\langle V_{(1,2)}^d \rangle}{\langle \psi_{(1,1)}^d \rangle} = \frac{\langle V_{(1,2)}^d \rangle}{\langle V_{(1,1)}^d \rangle}. \quad (2.18)$$

The first equality comes from using the OPE (1.5) in $\langle V_{(1,2)}^d \rangle$, taking into account $\langle \psi_{(1,3)}^d \rangle = 0$ (since $\Delta_{(1,3)} \neq 0$). The second equality comes from taking the bulk identity field to the boundary and producing the boundary identity. In the case of 1-point functions of degenerate fields, the shift equation therefore reads

$$\frac{\langle V_{(1,2)}^d \rangle}{\langle V_{(1,1)}^d \rangle} \langle V_{(1,s)}^d \rangle = \langle V_{(1,s+1)}^d \rangle + \langle V_{(1,s-1)}^d \rangle, \quad (2.19)$$

and the solution is

$$\langle V_{(1,s)}^d \rangle_\sigma = \frac{\sin(2\pi\beta^{-1}\sigma s)}{\sin(2\pi\beta^{-1}\sigma)} \langle V_{(1,1)}^d \rangle_\sigma, \quad (2.20)$$

where the disc partition function $\langle V_{(1,1)}^d \rangle_\sigma$ is left unconstrained.

It remains to determine whether the boundary is discrete or continuous, depending on the parameter σ . Knowing the disc 1-point function, we can use the modular bootstrap for deducing the boundary spectrum, see Section 2.4. Here we propose a technically simpler criterion, which relies on a plausible but unproven assumption:

$$\text{The boundary } \sigma \text{ is discrete} \iff \lim_{P \rightarrow P_{(r,s)}} \langle V_P \rangle_\sigma = \langle V_{(r,s)}^d \rangle_\sigma. \quad (2.21)$$

If the boundary is discrete, we indeed expect that the bulk-to-boundary OPE commutes with the limit $P \rightarrow P_{(r,s)}$. If it is continuous, however, the bulk-to-boundary OPE involves an integral over boundary momenta, and poles of the integrand may well cross or pinch the integration contour in the limit $P \rightarrow P_{(r,s)}$, leading to more subtle behaviour. Together with Eq. (2.18), our assumption (2.21) leads to the determination of the discrete values of σ in Eq. (1.10).

We can gain intuition about the behaviour of diagonal fields as they approach degenerate values by comparing with known results in Liouville theory. In Liouville theory with generic central charge $c \in \mathbb{C} \setminus (-\infty, 1]$, we have $\lim_{P \rightarrow P_{(r,s)}} V_P = V_{(r,s)}^d$ in bulk OPEs; what about in disc 1-point functions? Disc 1-point functions obey the shift equation (1.8), in a field normalisation such that $V_P = V_{-P}$. There exist discrete boundary conditions called Zamolodchikov–Zamolodchikov boundary conditions [16], parametrised by pairs of Kac indices $(m, n) \in (\mathbb{N}^*)^2$, and continuous boundary conditions called Fateev–Zamolodchikov–Zamolodchikov–Teschner boundary conditions [12, 17], parametrised by $\sigma \in \mathbb{C}$. Up to P -independent factors, the bulk 1-point functions and boundary cosmological constants are

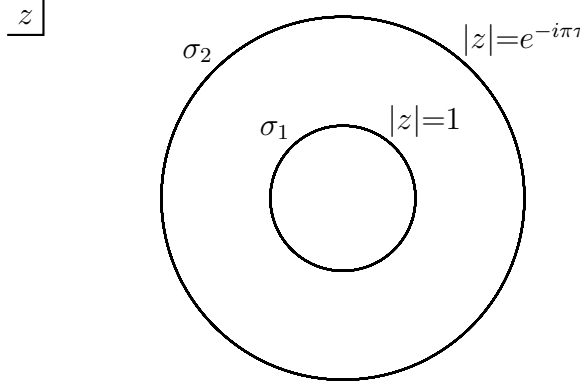
$$\text{ZZ: } \langle V_P \rangle_{(m,n)} = \sin(2\pi\beta m P) \sin(2\pi\beta^{-1} n P) \quad , \quad \mu_{(m,n)} = 2(-1)^m \cos(\pi\beta^{-2} n) \quad , \quad (2.22)$$

$$\text{FZZT: } \langle V_P \rangle_\sigma = \cos(4\pi\sigma P) \quad , \quad \mu_\sigma = 2 \cos(2\pi\beta^{-1}\sigma) \quad . \quad (2.23)$$

In fact, a ZZ boundary condition is a linear combination of two FZZT boundary conditions with boundary parameters $\sigma = P_{(m,\pm n)}$. Since these two parameters correspond to the same boundary cosmological constant $\mu_{(m,n)} = \mu_{P_{(m,n)}} = \mu_{P_{(m,-n)}}$, the corresponding boundary conditions can be combined without spoiling the shift equations. The 1-point functions for ZZ and FZZT boundary conditions agree with our criterion (1.10): μ is a ratio of 1-point functions in the ZZ case but not in the FZZT case, except for $\sigma = P_{(0,s)}$ with $s \in \mathbb{Z} + \frac{1}{2}$. And this exception would disappear if we also considered the shift equations from the second degenerate field $V_{(2,1)}^d$.

2.4 Modular bootstrap on the annulus

On an annulus, consider a critical loop model with boundary conditions σ_1 on the inner boundary and σ_2 on the outer boundary:



(2.24)

The corresponding annulus partition function can be computed in the bulk and boundary channels. The 2 channels are related by a modular transformation $\tau \rightarrow -\frac{1}{\tau}$, which will allow us to deduce the boundary spectrum from bulk structure constants.

We therefore start with the bulk channel. Since we are considering diagonal boundary conditions, only diagonal fields appear and we take the spectrum to be $\{V_P\}_{P \in P_0 + \beta^{-1}\mathbb{Z}}$, as in the bulk CFT [14]. The partition function in the boundary channel is constructed from disc 1-point functions and sphere 2-point functions as follows

$$Z_{\sigma_1, \sigma_2} = \sum_{P \in P_0 + \beta^{-1}\mathbb{Z}} \frac{\langle V_P \rangle_{\sigma_1} \langle V_P \rangle_{\sigma_2}}{B_P} \chi_P(\tau) \quad \text{with} \quad \chi_P(\tau) = \frac{e^{2\pi i \tau P^2}}{\eta(\tau)}, \quad (2.25)$$

where $\eta(\tau)$ is the Dedekind eta function. Using the expressions of the disc 1-point function $\langle V_P \rangle_{\sigma}$ (1.9) and sphere 2-point structure constant B_P (2.9), this is explicitly

$$Z_{\sigma_1, \sigma_2} = -\sin(\pi\beta^2) \sin(\pi\beta^{-2}) \sum_{P \in P_0 + \beta^{-1}\mathbb{Z}} \frac{\sin(4\pi\sigma_1 P) \sin(4\pi\sigma_2 P)}{\sin(2\pi\beta P) \sin(2\pi\beta^{-1} P)} \chi_P(\tau). \quad (2.26)$$

In order to rewrite this partition function in the boundary channel, we use the behaviour of the character under the modular transformation:

$$\chi_P(\tau) = \sqrt{2} \int_{-\infty}^{\infty} dP' \cos(4\pi P P') \chi_{P'}(-\frac{1}{\tau}). \quad (2.27)$$

This leads to $Z_{\sigma_1, \sigma_2} = \int_{-\infty}^{\infty} dP' \rho_{\sigma_1, \sigma_2}(P') \chi_{P'}(-\frac{1}{\tau})$: an integral over a continuous boundary spectrum, with the spectral density

$$\rho_{\sigma_1, \sigma_2}(P') = -\frac{\sqrt{2} \sin(\pi\beta^2) \sin(\pi\beta^{-2})}{\sin(2\pi P_0 \beta)} \sum_{P \in P_0 + \beta^{-1}\mathbb{Z}} \frac{\sin(4\pi\sigma_1 P) \sin(4\pi\sigma_2 P)}{\sin(2\pi P \beta^{-1})} \cos(4\pi P P'). \quad (2.28)$$

The integral collapses to a discrete sum if the density is a combination of delta functions. This happens if and only if the summand of $\sum_{P \in P_0 + \beta^{-1}\mathbb{Z}}$ is in fact trigonometric, due to the identity

$$\sum_{P \in P_0 + \beta^{-1}\mathbb{Z}} e^{4\pi i P P'} = -\frac{\beta}{2} e^{-4\pi i P_0 P_{(r,0)}} \sum_{r \in \mathbb{Z}} \delta(P' + P_{(r,0)}). \quad (2.29)$$

For the summand to be trigonometric, we need $\sigma_i = P_{(0,S_i)}$ with $S_i \in \mathbb{N}^*$ for $i = 1$ or $i = 2$. Then we can use the identity

$$\frac{\sin(S_1 x) \sin(S_2 x)}{\sin(x)} \stackrel{S_1 \in \mathbb{C}}{=} \sum_{\substack{S_2 \in \mathbb{N}^* \\ s \stackrel{2}{=} 1-S_2}}^{S_2-1} \sin((S_1 + s)x) \stackrel{S_1, S_2 \in \mathbb{N}^*}{=} \sum_{s \stackrel{2}{=} |S_1 - S_2| + 1}^{S_1 + S_2 - 1} \sin(sx). \quad (2.30)$$

If the second boundary is discrete, the partition function becomes

$$Z_{\sigma_1, S_2} = -\frac{\beta \sin(\pi\beta^2) \sin(\pi\beta^{-2})}{\sqrt{2} \sin(2\pi P_0 \beta)} \sum_{r \in \mathbb{Z}} \sum_{s \stackrel{2}{=} 1-S_2}^{S_2-1} \sin(2\pi r P_0 \beta) \chi_{\sigma_1 + P_{(r,s)}}(-\frac{1}{\tau}). \quad (2.31)$$

If the first boundary is also discrete, the characters combine into characters of degenerate representations $\chi_{(r,s)}^d = \chi_{P_{(r,s)}} - \chi_{P_{(r,-s)}}$, and we find

$$Z_{S_1, S_2} = -\frac{\beta \sin(\pi\beta^2) \sin(\pi\beta^{-2})}{\sqrt{2} \sin(2\pi P_0 \beta)} \sum_{r \in \mathbb{N}^*} \sum_{s \stackrel{2}{=} |S_1 - S_2| + 1}^{S_1 + S_2 - 1} \sin(2\pi r P_0 \beta) \chi_{(r,s)}^d(-\frac{1}{\tau}). \quad (2.32)$$

We therefore recover the condition (1.10) for the boundary to be discrete. Moreover, in the case $S_1 = S_2 = S$, we find the degenerate boundary spectrum \mathcal{S}_S (1.11).

3 Bulk 2-point functions on the disc

In this section we compute disc 2-point functions of the type $\langle V_{(r_1, s_1)} V_{(r_2, s_2)} \rangle_\sigma$, where $r_1 + r_2 \in \mathbb{N}$, and $\sigma \in \mathbb{C}$ is the parameter of a diagonal boundary. We use the notation $V_{(r,s)}$ not only for non-diagonal fields, but also for diagonal fields via the identification $V_P = V_{(0, 2\beta P)}$. Our 2-point function can be decomposed into conformal blocks in 2 ways:

- in the bulk channel using the OPE between the 2 bulk fields,
- in the boundary channel using bulk-to-boundary OPEs.

The agreement between the 2 decompositions is called crossing symmetry, and provides a non-trivial test of the bulk and boundary spectra, and of the disc 1-point function.

3.1 Bulk channel decomposition

While bulk OPEs in critical loop models are not known in general, let us argue that enough is known for computing our disc 2-point function. First, it is known that r is conserved modulo integers [5], therefore

$$\langle V_{(r_1, s_1)} V_{(r_2, s_2)} \rangle_\sigma \neq 0 \implies r_1 + r_2 \in \mathbb{N}. \quad (3.1)$$

In the following correlators and OPEs we assume $r_1 + r_2 \in \mathbb{N}$. Under this condition, diagonal fields can appear in the OPE $V_{(r_1, s_1)} V_{(r_2, s_2)}$. Such fields form a discrete infinite family $\{V_P\}_{P \in P_0 + \beta^{-1}\mathbb{Z}}$, characterised by the momentum P_0 .

We thus expect an OPE of the type

$$V_{(r_1, s_1)} V_{(r_2, s_2)} \sim \sum_{P \in P_0 + \beta^{-1}\mathbb{Z}} C_{(r_1, s_1)(r_2, s_2)}^P V_P + \sum_{r \in \mathbb{N}^*} \sum_{s \in \frac{1}{\tau}\mathbb{Z}} C_{(r_1, s_1)(r_2, s_2)}^{(r,s)} V_{(r,s)}, \quad (3.2)$$

where we write primary fields while omitting descendant fields. In CFT, we generally expect that OPE coefficients are related to 3-point and 2-point structure constants by the simple relation $C_{ij}^k = \frac{C_{ijk}}{B_k}$. However, in critical loop models, this relation does not hold in general. We know the 2-point and 3-point structure constants B_k, C_{ijk} [7], but they are not enough for computing sphere 4-point functions: extra factors are needed, which are polynomial in loop weights [6]. Nevertheless, these extra factors were found to be trivial whenever the channel field is diagonal. We therefore assume

$$C_{(r_1, s_1)(r_2, s_2)}^P = \frac{C_{(r_1, s_1)(r_2, s_2)P}}{B_P} = \lambda_P \frac{\tilde{C}_{(r_1, s_1)(r_2, s_2)P}}{B_P}, \quad (3.3)$$

where λ_P is the renormalisation factor (2.6), B_P is the 2-point structure constant in our normalisations (2.9), and $\tilde{C}_{(r_1, s_1)(r_2, s_2)P}$ is a 3-point structure constant in the normalisation of [7], namely

$$\tilde{C}_{(r_1, s_1)(r_2, s_2)(r_3, s_3)} = \prod_{\epsilon_1, \epsilon_2, \epsilon_3 = \pm} \Gamma_{\beta}^{-1} \left(\frac{\beta + \beta^{-1}}{2} + \frac{\beta}{2} |\sum_i \epsilon_i r_i| + \frac{\beta^{-1}}{2} \sum_i \epsilon_i s_i \right). \quad (3.4)$$

The explicit evaluation of $C_{(r_1, s_1)(r_2, s_2)}^P$ leads to the formula (1.14). When writing $\tilde{C}_{(r_1, s_1)(r_2, s_2)(r_3, s_3)}$ and deducing $C_{(r_1, s_1)(r_2, s_2)}^P$, we have neglected sign factors, which are in particular necessary to ensure the right behaviour under a permutation of the fields $V_{(r_1, s_1)}$ and $V_{(r_2, s_2)}$. However, such sign factors are P -independent, and will not affect our tests of crossing symmetry.

In the case of a 2-point function of diagonal fields $\langle V_{P_1} V_{P_2} \rangle_{\sigma}$, let us be more careful with normalisations: we renormalise the fields V_{P_1} and V_{P_2} in addition to the channel field V_P , and we also perform a field-independent renormalisation of \tilde{C} such that $C_{P_{(1,1)}, P_{(1,1)}}^{P_{(1,1)}} = 1$ is valid for identity fields:

$$C_{P_1, P_2}^P = \frac{\lambda_P \lambda_{P_1} \lambda_{P_2}}{\lambda_{P_{(1,1)}}^3} \frac{\tilde{C}_{P, P_1, P_2}}{\tilde{C}_{P_{(1,1)}, P_{(1,1)}, P_{(1,1)}}} \frac{1}{B_P}. \quad (3.5)$$

This normalisation will ensure agreement with the boundary structure constant $D_{(1,1)}$ (3.7).

We can now insert the bulk OPE (3.2) in our disc 2-point function, and deduce the bulk channel decomposition (1.12). Since our boundary condition is diagonal, only the diagonal terms of the bulk OPE contribute. The disc 2-point conformal blocks that appear are identical to sphere 4-point conformal blocks, which depend on the left-moving and right-moving dimensions $\Delta_{(r,s)}, \Delta_{(r,-s)}$ of each one of our 2 bulk fields. Such Virasoro conformal blocks are well-known and can be computed to arbitrary precision. In this sense, our bulk channel decomposition provides an explicit formula for disc 2-point functions.

In the case where our 2 bulk fields are diagonal, we may be tempted to compare our disc 2-point function $\langle V_{P_1} V_{P_2} \rangle_{\sigma}$ with the similar quantity in Liouville theory, which also depends on the continuous parameters P_1, P_2, σ, β . The relevant structure constants coincide with those of Liouville theory with $c \leq 1$ (sometimes called imaginary Liouville theory). The main differences with Liouville theory are:

- Our 2-point function is a discrete sum, while the Liouville 2-point function is an integral.
- In addition to Liouville theory, we have an extra continuous parameter P_0 .
- Loop models exist and are expected to be analytic over $\{\Re \beta^2 > 0\}$, while Liouville theory exists for $\beta^2 \in \mathbb{C}^*$ with, however, an essential singularity for $\beta^2 \in (0, \infty)$.

3.2 Boundary channel decomposition

We expect that the disc 2-point function has a boundary channel decomposition of the type (1.15), involving a sum over the boundary spectrum \mathcal{S}_σ , and structure constants D_k .

If the boundary is continuous, the sum is actually an integral, and we do not know the structure constants. With known numerical bootstrap methods, we cannot extract any information from the existence of the boundary channel decomposition. Therefore, the bulk channel decomposition remains an untested conjecture in this case.

From now on we focus on discrete boundaries, whose boundary parameters are $\sigma = P_{(0,S)}$ with $S \in \mathbb{N}^*$. We know the boundary spectrum (1.11), which is discrete, but we still do not know the structure constants D_k . Crossing symmetry is a linear system of equations for D_k , and the existence of solutions is a strong test of the boundary spectrum, and also of the bulk channel spectrum and structure constants.

Numerical results show that the boundary channel spectrum is a subset $\mathcal{S}_S^{r_1, r_2}$ (1.16) of the boundary spectrum, consistent with the bulk-to-boundary OPE (1.17). In particular, the boundary identity field $\psi_{\langle 1,1 \rangle}^d$ contributes to the boundary channel decomposition if and only if $r_1 = r_2 = 0$, in other words in the case of 2-point functions of diagonal fields $\langle V_{P_1} V_{P_2} \rangle_S$. In this case, we can compute the structure constant corresponding to $\psi_{\langle 1,1 \rangle}^d$ in terms of the disc 1-point function:

$$D_{\langle 1,1 \rangle} = \frac{\langle V_{P_1} \psi_{\langle 1,1 \rangle}^d \rangle_S \langle V_{P_2} \psi_{\langle 1,1 \rangle}^d \rangle_S}{\langle \psi_{\langle 1,1 \rangle}^d \psi_{\langle 1,1 \rangle}^d \rangle_S} = \frac{\langle V_{P_1} \rangle_S \langle V_{P_2} \rangle_S}{\langle V_{\langle 1,1 \rangle}^d \rangle_S} = \frac{\langle V_{P_1} \rangle_S \langle V_{P_2} \rangle_S}{\langle V_{P_{(1,1)}} \rangle_S}. \quad (3.6)$$

The first equality comes from taking the bulk fields to the boundary and producing the identity field. In the second equality we used the fact that $\psi_{\langle 1,1 \rangle}^d$ and $V_{\langle 1,1 \rangle}^d$ are identity fields and in the third equality the characterisation (2.21) of discrete boundaries was used to swap the identity field for a diagonal field with momentum $P_{(1,1)}$. With our disc 1-point function (1.9), this leads to

$$D_{\langle 1,1 \rangle} = \frac{\sin(2\pi\beta^{-1}SP_1) \sin(2\pi\beta^{-1}SP_2)}{(-1)^S \sin(\pi\beta^{-2}S)}. \quad (3.7)$$

3.3 Numerical bootstrap results

Numerical bootstrap methods for sphere 4-point functions in 2d CFTs with exactly known spectra are reviewed in [5]. We have adapted these methods to disc 2-point functions. We assume that the bulk and boundary spectra are known and discrete, as we would not know how to safely truncate a continuous spectrum to make it finite: this is why we are focussing on discrete boundaries. For a disc 2-point functions, the conformal blocks should in principle be evaluated for values of the cross-ratio $z = \left| \frac{z_1 - z_2}{z_1 - \bar{z}_2} \right|^2 \in (0, 1)$. By analyticity, crossing symmetry in fact holds for any $z \in \mathbb{C} \setminus \{0, 1\}$, and we find it numerically convenient to use complex values of z .

Crossing symmetry is then a system of linear equations for the bulk and boundary channel structure constants. We can numerically determine the dimension of the space of solutions, and the structure constants for specific solutions. In practice we focus on cases when the solution is unique, by fixing the values of some structure constants and/or by restricting the boundary spectrum.

We will now state the main results that we obtained numerically. We state the results as general conjectures, which we tested for a finite number of cases with $\beta = 0.8 + 0.1i$, and found to hold in all these cases.

Claim 1. Given the bulk channel decomposition (1.12) and boundary spectrum \mathcal{S}_S (1.11), there is a unique solution to the crossing equation (1.12) = (1.15).

We tested this claim with boundary parameters $S \in \{1, 2, 3\}$ and bulk channel momentum $P_0 = P_{(0, \frac{1}{17})}$, for the following disc 2-point functions:

$$\begin{aligned} & \left\langle V_{P_{(0, \frac{1}{15})}} V_{P_{(0, \frac{1}{16})}} \right\rangle, \left\langle V_{P_{(0, \frac{1}{15})}} V_{(1,0)} \right\rangle, \left\langle V_{(1,0)} V_{(1,0)} \right\rangle, \left\langle V_{(\frac{1}{2},0)} V_{(\frac{3}{2}, \frac{2}{3})} \right\rangle, \left\langle V_{(\frac{1}{2},2)} V_{(\frac{1}{2},2)} \right\rangle, \\ & \left\langle V_{P_{(0, \frac{1}{15})}} V_{(2,0)} \right\rangle, \left\langle V_{(2, \frac{1}{2})} V_{(2, -\frac{1}{2})} \right\rangle, \left\langle V_{(3, \frac{2}{3})} V_{(3, \frac{1}{3})} \right\rangle, \left\langle V_{(1,1)} V_{(3, \frac{1}{3})} \right\rangle, \left\langle V_{(2, \frac{1}{2})} V_{(3, \frac{2}{3})} \right\rangle, \\ & \left\langle V_{(\frac{1}{2},0)} V_{(\frac{1}{2},0)} \right\rangle, \left\langle V_{(\frac{1}{2},0)} V_{(\frac{3}{2},0)} \right\rangle, \left\langle V_{(\frac{1}{2},0)} V_{(\frac{5}{2},0)} \right\rangle, \left\langle V_{(\frac{3}{2},0)} V_{(\frac{3}{2},0)} \right\rangle, \left\langle V_{(\frac{3}{2},0)} V_{(\frac{5}{2},0)} \right\rangle. \end{aligned} \quad (3.8)$$

Claim 2. For this solution, $D_{\langle r,s \rangle} = 0$ if $r \leq 2 \max(r_1, r_2)$ or if $r \equiv 2r_1 \pmod{2}$. Therefore the boundary spectrum is $\mathcal{S}_S^{r_1, r_2} \subset \mathcal{S}_S$ (1.16).

(Notice that $2r_1 \equiv 2r_2 \pmod{2}$ due to Eq. (3.1).) To give a quantitative idea of our evidence for this claim, we focus on the non-vanishing boundary structure constant with the lowest Kac indices $D_{\min} = D_{\langle 2 \max(r_1, r_2) + 1, 1 \rangle}$. For this structure constant we display the deviation: an estimate of the relative error of the numerical bootstrap result with respect to the true value [5]. If claim 2 is true we expect small deviations; if it was wrong the deviations would typically be no smaller than about 10^{-3} . Our numerical calculations use numbers with 100 decimal digits, and the spectrum is truncated to a maximum conformal dimension of 80.

2-point function	D_{\min}	Deviation		
		$S = 1$	$S = 2$	$S = 3$
$\left\langle V_{(\frac{1}{2},2)} V_{(\frac{1}{2},2)} \right\rangle$	$D_{\langle 2,1 \rangle}$	10^{-29}	10^{-19}	10^{-6}
$\left\langle V_{(\frac{1}{2},2)} V_{(\frac{3}{2}, \frac{2}{3})} \right\rangle$	$D_{\langle 4,1 \rangle}$	10^{-34}	10^{-25}	10^{-10}
$\left\langle V_{(\frac{3}{2}, \frac{2}{3})} V_{(\frac{3}{2}, \frac{2}{3})} \right\rangle$	$D_{\langle 4,1 \rangle}$	10^{-37}	10^{-26}	10^{-8}
$\left\langle V_{(1,0)} V_{(1,0)} \right\rangle$	$D_{\langle 3,1 \rangle}$	10^{-45}	10^{-32}	10^{-11}
$\left\langle V_{(1,0)} V_{(2,0)} \right\rangle$	$D_{\langle 5,1 \rangle}$	10^{-43}	10^{-31}	10^{-13}
$\left\langle V_{(2,0)} V_{(2,0)} \right\rangle$	$D_{\langle 5,1 \rangle}$	10^{-41}	10^{-31}	10^{-13}

In some examples, we find more structure constants that vanish, and the boundary spectrum becomes even smaller. In the cases of $\left\langle V_{(\frac{1}{2},0)} V_{(\frac{1}{2},0)} \right\rangle$, $\left\langle V_{(\frac{1}{2},0)} V_{(\frac{3}{2},0)} \right\rangle$ and $\left\langle V_{(\frac{3}{2},0)} V_{(\frac{3}{2},0)} \right\rangle$ with $S = 2, 3$, we indeed find $D_{\langle r,3 \rangle} = 0$. Understanding this observation is left for future work.

Claim 3. In the case of $\langle V_{P_1} V_{P_2} \rangle_S$, the value of $D_{\langle 1,1 \rangle}$ is given by Eq. (3.7).

In a few cases, let us display the error, i.e. the relative difference of our analytic prediction with the numerical result for $D_{\langle 1,1 \rangle}$. Claim 3 implies that the errors should be

small, and should decrease when the numerical precision is improved. Numerical results are consistent with these expectations.

2-point function	Error		
	$S = 1$	$S = 2$	$S = 3$
$\langle V_{P_{(0, \frac{1}{12})}} V_{P_{(0, \frac{1}{13})}} \rangle$	10^{-45}	10^{-30}	10^{-10}
$\langle V_{P_{(0, \frac{1}{22})}} V_{P_{(0, \frac{1}{23})}} \rangle$	10^{-44}	10^{-30}	10^{-9}
$\langle V_{P_{(0, \frac{1}{9})}} V_{P_{(0, \frac{1}{17})}} \rangle$	10^{-45}	10^{-30}	10^{-10}

(3.10)

Claim 4. Given the bulk spectrum $\{V_P\}_{P \in P_0 + \beta^{-1}\mathbb{Z}}$ and the boundary spectrum $\mathcal{S}_{[s_0]}^{r_1, r_2} = \{\psi_{\langle r, s_0 \rangle}^d\}_{r \in 2 \max(r_1, r_2) + 1 + 2\mathbb{N}}$ with $s_0 \in 2\mathbb{N} + 1$, there exists a unique solution of crossing symmetry. We call this solution $\langle V_{(r_1, s_1)} V_{(r_2, s_2)} \rangle_{[s_0]}$.

We tested this claim with $s_0 \in \{1, 3, 5\}$ and bulk channel momentum $P_0 = P_{(0, \frac{1}{17})}$, for the disc 2-point functions (3.8).

Compared to $\langle V_{(r_1, s_1)} V_{(r_2, s_2)} \rangle_S$, the solutions $\langle V_{(r_1, s_1)} V_{(r_2, s_2)} \rangle_{[s_0]}$ have smaller boundary spectra. The bulk channel decomposition is still of the type (1.12), but the coefficients are now unknown, rather than having the specific values $C_{(r_1, s_1)(r_2, s_2)}^P \langle V_P \rangle_\sigma$. These 2 families of solutions are however related:

Claim 5. The solution $\langle V_{(r_1, s_1)} V_{(r_2, s_2)} \rangle_S$ is a linear combination of $\langle V_{(r_1, s_1)} V_{(r_2, s_2)} \rangle_{[s_0]}$ with $s_0 = 1, 3, \dots, 2S - 1$.

Equivalently, the ratios of boundary structure constants $\frac{D_{\langle r, s \rangle}}{D_{\langle r', s \rangle}}$ do not depend on the boundary parameter S , since they are determined by the solutions $\langle V_{(r_1, s_1)} V_{(r_2, s_2)} \rangle_{[s_0]}$. In other words, there exist shift equations for the dependence on the first Kac index r .

Our claim implies that the following quantity should vanish:

$$\text{Error} = \left| 1 - \frac{D_{\langle r', 1 \rangle}^{(S)} D_{\langle r, 1 \rangle}^{(S=1)}}{D_{\langle r, 1 \rangle}^{(S)} D_{\langle r', 1 \rangle}^{(S=1)}} \right|. \quad (3.11)$$

We now display the order of magnitude of the error, when numerically computed for a

couple of 2-point functions. We find errors that are close to zero, supporting our claim:

$$\left\langle V_{P_{(0, \frac{1}{15})}} V_{P_{(0, \frac{1}{16})}} \right\rangle \quad \left\langle V_{(1,0)} V_{(1,0)} \right\rangle$$

(r, s)	Error		(r, s)	Error	
	$S = 2$	$S = 3$		$S = 2$	$S = 3$
$(3, 1)$	10^{-31}	10^{-10}	$(5, 1)$	10^{-28}	10^{-8}
$(5, 1)$	10^{-30}	10^{-9}	$(7, 1)$	10^{-27}	10^{-7}
$(7, 1)$	10^{-29}	10^{-8}	$(9, 1)$	10^{-24}	10^{-6}
$(9, 1)$	10^{-26}	10^{-6}	$(11, 1)$	10^{-21}	10^{-5}

(3.12)

In addition to these 2 examples, we have tested our claim in the following cases, with similar results:

$$\begin{aligned} & \left\langle V_{(1,1)} V_{(1,1)} \right\rangle, \left\langle V_{(1,1)} V_{(3, \frac{1}{3})} \right\rangle, \left\langle V_{(2,1)} V_{(2, \frac{1}{2})} \right\rangle, \left\langle V_{(2,0)} V_{(3,0)} \right\rangle, \\ & \left\langle V_{P_{(0, \frac{1}{5})}} V_{(1,1)} \right\rangle, \left\langle V_{P_{(0, \frac{1}{7})}} V_{(3, \frac{1}{3})} \right\rangle, \left\langle V_{P_{(0, \frac{1}{8})}} V_{(2,0)} \right\rangle, \left\langle V_{P_{(0, \frac{1}{9})}} V_{(2, \frac{1}{2})} \right\rangle. \end{aligned}$$

We have also done more direct checks of claim 5. Namely, we have numerically solved the following system of linear equations, where the unknowns are $D_{\langle r, s_0 \rangle}$ and c_S :

$$\sum_{r \stackrel{2}{=} 2\max(r_1, r_2)+1}^{\infty} D_{\langle r, s_0 \rangle} \begin{array}{c} (r_1, s_1) \quad (r_2, s_2) \\ \diagdown \quad \diagup \\ \langle r, s_0 \rangle \\ \diagup \quad \diagdown \\ (r_1, -s_1) \quad (r_2, -s_2) \end{array} = \sum_{S=1}^{\frac{s_0+1}{2}} c_S \left\langle V_{(r_1, s_1)} V_{(r_2, s_2)} \right\rangle_S. \quad (3.13)$$

Here the left-hand side is the boundary channel decomposition of $\langle V_{(r_1, s_1)} V_{(r_2, s_2)} \rangle_{[s_0]}$, while on the right-hand side the 2-point functions $\langle V_{(r_1, s_1)} V_{(r_2, s_2)} \rangle_S$ are assumed to be known from their bulk channel decompositions (1.12). We find that the solution of this linear system is unique. Moreover, since the sum on the left-hand side is over only one index, and the sum on the right-hand side is finite, the number of unknowns, $D_{\langle r, s_0 \rangle}$ and c_S , is relatively small, after we make the system finite by truncating to a maximum conformal dimension in both channels. This allows us to test a rather large number of boundary channel structure constants $D_{\langle r, s \rangle}$. For example, in the case of $\left\langle V_{P_{(0, \frac{1}{13})}} V_{P_{(0, \frac{1}{14})}} \right\rangle_{[7]}$, we obtain deviations of the order of 10^{-8} for $D_{\langle 7, 7 \rangle}$ and $D_{\langle 9, 7 \rangle}$. (Deviations are even smaller than that for $s_0 = 3, 5$.)

4 Outlook

Diagonal and non-diagonal boundaries in lattice loop models

While we have borrowed terminology and used some intuition from loop models, our analysis was done purely in the bootstrap formalism. As usual with this axiomatic formalism,

a separate analysis is needed for identifying the physical systems that our results describe. We will now sketch some diagonal and non-diagonal boundary conditions in lattice loop models. A more complete analysis is left for future work.

The simplest boundary in loop models is called a free boundary. Such a boundary does not change any property of the model, except the geometry on which it is defined. It turns out that a free boundary corresponds to our discrete diagonal boundary with parameter $S = 1$: this is shown by computing the corresponding annulus partition function, which can be done either by combining lattice and field-theory methods [18, 19], or by using rigorous probability theory [20]. In any case, the result agrees with our partition function $Z_{1,1}$ (2.32).

To construct non-free boundaries, a simple possibility is to play with the weights of loops. In bulk loop models, contractible loops have weight $n = -2 \cos(\pi\beta^2)$. In boundary loop models, we can assign a different weight to loops that touch the boundary. Weight-modifying boundaries were studied in [21, 22, 23] in an algebraic framework based on the Temperley–Lieb algebra. This involved an idempotent blob generator that modifies the weights of loops touching the boundary, irrespective of how many times they touch it. The resulting annulus partition functions do not agree with our partition function Z_{σ_1, σ_2} (2.25): rather, they include terms that have non-vanishing couplings to non-diagonal fields. We conclude that weight-modifying boundaries are non-diagonal. Moreover, there exist Dirichlet boundaries where loops can end [21]: such boundaries are also non-diagonal.

We can also build non-free, diagonal boundaries using the ideas of [21, 22, 23]. To do this, we cannot simply modify loop weights: we have to modify finer microscopic properties of lattice loop models. The required modifications depend on whether the model is in a dense or dilute phase, corresponding respectively to $0 < \beta^2 < 1$ or $1 < \beta^2 \leq 2$.

- In the dense phase, let us build a lattice with 2 boundaries by the time evolution of an open spin chain with $2N$ sites. The loop model’s evolution is described by a transfer matrix, written in terms of the generators $1, e_1, e_2, \dots, e_{2N-1}$ of the Temperley–Lieb algebra $\text{TL}_{2N}(n)$. With free boundaries, the transfer matrix is

$$T_1 = \prod_{i=2}^{2N-2} (1 + e_i) \prod_{i=1}^{2N-1} (1 + e_i) . \quad (4.1)$$

For a diagonal boundary with parameter $S \geq 2$ on the left of the chain, we propose that the factors with $1 \leq i \leq S - 1$ should be replaced with the Jones–Wenzl projector P_S [24]. This leads to the transfer matrix

$$T_S = P_S \prod_{i=2 \lfloor \frac{S+1}{2} \rfloor}^{2N-2} (1 + e_i) \prod_{i=1+2 \lfloor \frac{S}{2} \rfloor}^{2N-1} (1 + e_i) , \quad (4.2)$$

where $P_2 = 1 - \frac{1}{n}e_1$, and more generally P_S is the unique element of $\text{TL}_S(n)$ satisfying $P_S^2 = P_S$ and $e_i P_S = P_S e_i = 0$ for $i = 1, 2, \dots, S - 1$. The agreement with the CFT’s annulus partition function Z_{S_1, S_2} (2.32) boils down to a relation of the type

$$\lim_{\text{critical}} \text{Tr} T_S^M = Z_{S,1} , \quad (4.3)$$

where the modulus of the annulus is given in terms of the lattice parameters by $\tau = \lim_{\text{critical}} i \frac{M}{2N}$. The case $S = 2$ extends to generic values of $Q = n^2$ a boundary condition that first appeared in the $Q = 3$ -state Potts model under the name “new”

[25]. We can similarly define a transfer matrix such that $\lim_{\text{critical}} \text{Tr } T_{S_1, S_2}^M = Z_{S_1, S_2}$:

$$T_{S_1, S_2} = P_{S_1}^{\text{left}} P_{S_2}^{\text{right}} \prod_{i=2\lfloor \frac{S_1+1}{2} \rfloor}^{2N-2\lfloor \frac{S_2+1}{2} \rfloor} (1+e_i) \prod_{i=1+2\lfloor \frac{S_1}{2} \rfloor}^{2N-1-2\lfloor \frac{S_2}{2} \rfloor} (1+e_i), \quad (4.4)$$

where $P_{S_1}^{\text{left}}$ projects on the first S_1 sites as before, whereas $P_{S_2}^{\text{right}}$ now projects on the last S_2 sites.

- In the dilute phase, in order to build a non-free boundary, we need to force loops to explore the boundary often enough. To do this, we can modify the monomer weight K : one of the two parameters of the loop model, together with the loop weight n . The critical limit corresponds to a critical value K_c , with $K_c = \frac{1}{\sqrt{2+\sqrt{2-n}}}$ on a hexagonal lattice [26]. In the presence of a boundary, we can however give a different weight to boundary monomers, and the critical limit depends on that boundary weight. There is a value $K_s > K_c$ such that we obtain free boundary conditions for any boundary weight $K < K_s$, and different boundary conditions called special for $K = K_s$ [27, 28], with $K_s = (2-n)^{-\frac{1}{4}}$ on a hexagonal lattice [29]. We now claim that in the resulting CFT, the free and special boundary conditions correspond to discrete diagonal boundaries with $S = 1$ and $S = 2$ respectively. As in the dilute case, this claim is supported by computing the annulus partition function, and comparing with the CFT result Z_{S_1, S_2} (2.32).

These constructions suggest that a boundary is diagonal if and only if it preserves the global symmetry of the loop model. The $O(n)$, Potts and $PSU(n)$ loop models indeed have global symmetries that include (but are much larger than) the groups $O(n)$, S_Q and $PSU(n)$ [30]. These global symmetries commute with the Jones–Wenzl projector that we used in the dense case, and are left unbroken by modifying the weights of boundary monomers as we did in the dilute case. On the other hand, the blob generator of weight-modifying boundaries breaks these symmetries. On the CFT side, diagonal fields are global symmetry singlets, whereas non-diagonal fields transform in non-trivial representations [31, 32].

Combinatorial description of correlation functions

In bulk critical loop models, correlation functions are parametrised by combinatorial maps [15]. We expect that this remains true in the presence of boundaries. In the case of bulk 2-point functions on the disc with a discrete diagonal boundary, our results agree with this expectation. For example, in the case of the 2-point function $\langle V_{(\frac{3}{2}, 0)} V_{(\frac{1}{2}, 0)} \rangle$, the fields that appear have 3 legs and 1 leg respectively, leading to a unique combinatorial map on the disc:



The uniqueness of this map corresponds to the uniqueness of the solution of crossing symmetry for this 2-point function. At the combinatorial level, the problem can be mapped to the sphere, by replacing the disc's boundary with a legless vertex. A disc

with 2 vertices (whose total number of legs is even) gives rise to a unique map, just like a sphere with 3 vertices. More generally, we have the equivalence

$$\left\langle \prod_{i=1}^N V_{(r_i, s_i)} \right\rangle^{\text{disc with diagonal boundary}} \underset{\text{combinatorially}}{\simeq} \left\langle V_P \prod_{i=1}^N V_{(r_i, s_i)} \right\rangle^{\text{sphere}}. \quad (4.6)$$

This allows us to predict the dimension of the space of solutions of crossing symmetry, for any correlation function of bulk fields on the disc.

Further bootstrap challenges

Having determined disc 1-point functions for diagonal boundaries, we think we understand the space of such boundaries, with its coordinate $\sigma \in \mathbb{C}$. We can compute disc 2-point functions of bulk fields in the bulk channel, and we could compute disc N -point functions if we knew the bulk OPE. In order to solve critical loop models on the disc, we still need to understand boundary fields and the associated structure constants: the bulk-boundary 2-point structure constant, and the boundary 3-point structure constant. This problem can be addressed with the bootstrap method, analytic and numerical.

Then there is the challenge of non-diagonal boundaries. This is more difficult than the diagonal case, because we do not have a shift equation that would constrain how the disc 1-point function $\langle V_{(r,0)} \rangle$ depends on r . Moreover, since legs can end at the boundary or touch the boundary, the combinatorics predict large numbers of solutions of crossing symmetry.

We may look for hints of the existence and properties of non-diagonal boundaries in the annulus partition functions of [23]. These partition functions depend on several continuous parameters: the weights of various types of loops, depending on their topology and on whether or not they touch the boundaries. For generic values of the parameters, in the bulk-channel decomposition of the partition function, there are contributions from non-diagonal fields $V_{(r,0)}$ and also from degenerate fields including $V_{(1,2)}^d$. If we could factorise the annulus partition function into disc 1-point functions, this would contradict Eq. (1.7). However, in the presence of non-diagonal fields, we know that bulk OPEs are problematic, which suggests that we cannot deduce disc 1-point functions from annulus partition functions. Nevertheless, since we do know partition functions for an annulus with diagonal boundaries, we can conclude that the boundaries of [23] are generically non-diagonal.

Acknowledgements

- We are grateful to Paul Roux, Xin Sun and Gérard Watts for stimulating discussions.
- We thank Gérard Watts au Paul Roux for carefully reading a draft version of the manuscript and providing useful comments.
- RN thanks IPhT for hospitality when part of this work was done.
- MD is supported by the French Agence Nationale de la Recherche (ANR) under grant ANR-21-CE40-0003 (project CONFICA).

References

- [1] [Jacobsen, Jesper Lykke](#) (2009 book chapter)
Conformal Field Theory Applied to Loop Models (2)
- [2] [J. L. Cardy](#) (2005 review) [arXiv:cond-mat/0503313]
SLE for theoretical physicists. *Annals Phys.* 318 pp. 81–118 (2, 6)
- [3] [G. F. Lawler](#) (2007 review) [arXiv:0712.3256]
Schramm–Loewner Evolution (2)
- [4] [S. Sheffield](#) (2006) [arXiv:math/0609167]
Exploration trees and conformal loop ensembles (2)
- [5] [S. Ribault](#) (2024) [arXiv:2411.17262]
Exactly solvable conformal field theories (2, 3, 6, 7, 8, 9, 13, 15, 16)
- [6] [R. Nivesvivat, S. Ribault, J. L. Jacobsen](#) (2024) [arXiv:2311.17558]
Critical loop models are exactly solvable. *SciPost Physics* 17(2) (2, 5, 6, 14)
- [7] [J. L. Jacobsen, R. Nivesvivat, S. Ribault, P. Roux](#) (2025) [arXiv:2510.04701]
Three-point functions in critical loop models (2, 5, 14)
- [8] [J. L. Cardy](#) (1992) [arXiv:hep-th/9111026]
Critical percolation in finite geometries. *J. Phys. A* 25 pp. L201–L206 (2)
- [9] [O. Schramm](#) (2001) [arXiv:math/0107096]
A percolation formula. *Elect. Comm. Prob.* 6 pp. 115—120 (2)
- [10] [D. C. Lewellen](#) (1992)
Sewing constraints for conformal field theories on surfaces with boundaries. *Nucl. Phys. B* 372 pp. 654–682 (3, 5)
- [11] [T. Bautista, A. Bawane](#) (2022) [arXiv:2111.04715]
Boundary timelike Liouville theory: Bulk one-point and boundary two-point functions. *Phys. Rev. D* 106(12) p. 126011 (4)
- [12] [V. Fateev, A. B. Zamolodchikov, A. B. Zamolodchikov](#) (2000) [arXiv:hep-th/0001012]
Boundary Liouville field theory. I: Boundary state and boundary two-point function (4, 11)
- [13] [R. A. Janik](#) (2001) [arXiv:hep-th/0109021]
Exceptional boundary states at $c = 1$. *Nucl. Phys. B* 618 pp. 675–688 (5)
- [14] [S. Ribault](#) (2022) [arXiv:2209.09706]
Diagonal fields in critical loop models (5, 12)
- [15] [L. Grans-Samuelsson, J. L. Jacobsen, R. Nivesvivat, S. Ribault, H. Saleur](#) (2023) [arXiv:2302.08168]
From combinatorial maps to correlation functions in loop models. *SciPost Phys.* 15 p. 147 (6, 20)
- [16] [A. B. Zamolodchikov, A. B. Zamolodchikov](#) (2001) [arXiv:hep-th/0101152]
Liouville field theory on a pseudosphere (11)

- [17] [J. Teschner](#) (2000) [[arXiv:hep-th/0009138](#)]
Remarks on Liouville theory with boundary. PoS tmr2000 p. 041 (11)
- [18] M. Bauer, H. Saleur (1989)
On some relations between local height probabilities and conformal invariance. Nucl. Phys. B 320 pp. 591–624 (19)
- [19] [J. Cardy](#) (2006) [[arXiv:math-ph/0604043](#)]
The $O(n)$ model on the annulus. J. Stat. Phys. 125 pp. 1–21 (19)
- [20] [M. Ang](#), [G. Rémy](#), [X. Sun](#) (2025) [[arXiv:2203.12398](#)]
The moduli of annuli in random conformal geometry. Ann. Sci. École Norm. Sup. (19)
- [21] [J. L. Jacobsen](#), [H. Saleur](#) (2008) [[arXiv:math-ph/0611078](#)]
Conformal boundary loop models. Nucl. Phys. B 788 pp. 137–166 (19)
- [22] [J. L. Jacobsen](#), [H. Saleur](#) (2007) [[arXiv:0709.0812](#)]
Combinatorial aspects of boundary loop models. Journal of Statistical Mechanics: Theory and Experiment 2008(01) p. P01021 (19)
- [23] [J. Dubail](#), [J. L. Jacobsen](#), [H. Saleur](#) (2009) [[arXiv:0812.2746](#)]
Conformal two-boundary loop model on the annulus. Nuclear Physics B 813(3) (19, 21)
- [24] [S. Morrison](#) (2015) [[arXiv:1503.00384](#)]
A formula for the Jones-Wenzl projections (19)
- [25] [I. Affleck](#), [M. Oshikawa](#), [H. Saleur](#) (1998) [[doi:10.1088/0305-4470/31/28/003](#)]
Boundary critical phenomena in the three-state Potts model. Journal of Physics A: Mathematical and General 31(28) p. 5827 (20)
- [26] [B. Nienhuis](#) (1982) [[doi:10.1103/PhysRevLett.49.1062](#)]
Exact critical point and critical exponents of $O(n)$ models in two dimensions. Phys. Rev. Lett. 49 pp. 1062–1065 (20)
- [27] J. L. Cardy (1984)
Conformal invariance and surface critical behavior. Nucl. Phys. B 240 pp. 514–532 (20)
- [28] [P. Fendley](#), [H. Saleur](#) (1994) [[arXiv:cond-mat/9403095](#)]
Exact theory of polymer adsorption in analogy with the Kondo problem. Journal of Physics A: Mathematical and General 27(21) (20)
- [29] [M. T. Batchelor](#), [C. M. Yung](#) (1995) [[arXiv:cond-mat/9507010](#)]
Surface critical behavior of the honeycomb $O(n)$ loop model with mixed ordinary and special boundary conditions. J. Phys. A 28 pp. L421–L426 (20)
- [30] [N. Read](#), [H. Saleur](#) (2007) [[arXiv:cond-mat/0701259](#)]
Enlarged symmetry algebras of spin chains, loop models, and S -matrices. Nucl. Phys. B 777 pp. 263–315 (20)
- [31] [J. L. Jacobsen](#), [S. Ribault](#), [H. Saleur](#) (2023) [[arXiv:2208.14298](#)]
Spaces of states of the two-dimensional $O(n)$ and Potts models. SciPost Phys. 14 p. 092 (20)

- [32] [P. Roux, J. L. Jacobsen, S. Ribault, H. Saleur](#) (2025) [arXiv:2404.01935]
Critical spin chains and loop models with $PSU(n)$ symmetry. SciPost Physics 18(1)
(20)